

## Ergodicity Breaking Provably Robust to Arbitrary Perturbations

David T. Stephen<sup>1,2</sup>, Oliver Hart<sup>1</sup>, and Rahul M. Nandkishore<sup>1</sup>

<sup>1</sup>*Department of Physics and Center for Theory of Quantum Matter, University of Colorado Boulder, Boulder, Colorado 80309, USA*

<sup>2</sup>*Department of Physics, California Institute of Technology, Pasadena, California 91125, USA*

 (Received 3 October 2022; revised 13 February 2023; accepted 25 October 2023; published 23 January 2024)

We present a new route to ergodicity breaking via Hilbert space fragmentation that displays an unprecedented level of robustness. Our construction relies on a single emergent (prethermal) conservation law. In the limit when the conservation law is exact, we prove the emergence of Hilbert space fragmentation with an exponential number of frozen configurations. These configurations are low-entanglement states in the middle of the energy spectrum and therefore constitute examples of quantum many-body scars. We further prove that every frozen configuration is absolutely stable to arbitrary perturbations, to all finite orders in perturbation theory. In contrast to previous constructions, our proof is not limited to symmetric perturbations, or to perturbations with compact support, but also applies to perturbations with long-range tails, and even to arbitrary geometrically nonlocal  $k$ -body perturbations, as long as  $k/L \rightarrow 0$  in the thermodynamic limit, where  $L$  is linear system size. Additionally, we identify one-form  $U(1)$  charges characterizing some nonfrozen sectors, and discuss the dynamics starting from typical initial conditions, which we argue is best interpreted in terms of the magnetohydrodynamics of the emergent one-form symmetry.

DOI: [10.1103/PhysRevLett.132.040401](https://doi.org/10.1103/PhysRevLett.132.040401)

When do quantum many-body systems break ergodicity, and fail to reach thermal equilibrium under their own dynamics? “Traditional” answers have included integrable [1] and many-body localized [2,3] systems, both of which have extensively many conserved quantities. A more recent answer involves many-body scars [4–7], whereby typical initial conditions thermalize, but there exist special (low-entanglement) initial conditions that do not. More recently still, it was observed that the interplay of (finitely many) conservation laws can break ergodicity [8], a phenomenon that was later understood as arising from Hilbert space fragmentation (also known as shattering) [9,10], whereby the unitary time evolution matrix block diagonalizes into exponentially many subsectors, with the dynamics unable to connect different subsectors [11–17].

An important open question involves how *robust* ergodicity breaking is to perturbations. For integrable systems, and most systems hosting scars, it is not known if there is any class of perturbations to which the phenomenon is robust. Many-body localization has a proof of robustness [18], but the proof is subtle, only works for short-range interacting systems (with at most exponential tails) in one spatial dimension, and even there has recently been called into question [19]. In contrast, the best-studied route to Hilbert space fragmentation (charge and dipole conservation) has a simple proof of robustness [9] that applies in arbitrary dimensions, but only to symmetry-respecting perturbations with bounded spatial range. It is also known, however, that if conservation laws are implemented *emergently*, as prethermal conservation laws [20], then the

requirement that perturbations respect the corresponding symmetries gets lifted. Thus, it is known how to obtain (prethermal) Hilbert space fragmentation that is robust to perturbations with bounded spatial range. There are, however, two important shortcomings of this construction: (i) typical frozen states are given dynamics at some *finite* order in perturbation theory, (ii) if the restriction of bounded spatial range is removed, there exist simple four-body perturbations that melt frozen configurations.

In this Letter, we present a new route to ergodicity breaking via Hilbert space fragmentation that is *provably* robust to *any* perturbations, *without* the requirement that perturbations have bounded spatial range, and whose frozen configurations are *all* absolutely stable [21] to all orders in perturbation theory. Similarly to Refs. [9,16,17], we rely on prethermal (i.e., “emergent”) implementation of conservation laws to obtain exponentially many “frozen” configurations. These correspond to low-entanglement states in the middle of the spectrum, such that they are examples of many-body scars. Our proofs apply to fully geometrically nonlocal perturbations, as long as the perturbations are  $k$  body (i.e., act on no more than  $k$  qubits) with  $k/L \rightarrow 0$  in the thermodynamic limit, where  $L$  is linear system size. This includes physically realistic long-range interactions with power-law tails. As such, our construction produces ergodicity breaking with an unprecedented degree of robustness, and opens a new direction for the study of nonergodic quantum dynamics. The phenomenon, moreover, arises in a system with a “generalized Rydberg” constraint, which could plausibly be accessed in

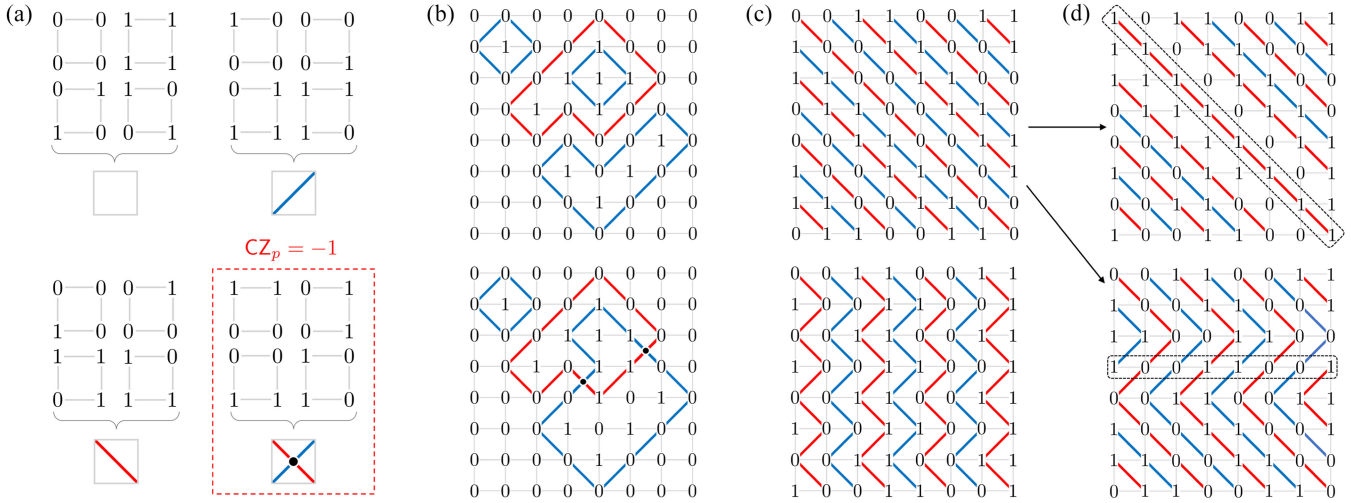


FIG. 1. (a) Configurations of spins around a plaquette grouped by their image under the duality mapping. The blue (red) lines indicate domain walls of the even (odd) sublattice. Forbidden configurations of spins with  $\text{CZ}_p = -1$ , corresponding to intersecting loops, are marked by the dotted box. (b) Configurations of spins are displayed with their corresponding image under the duality mapping. The upper configuration is allowed in the restricted Hilbert space while the lower is not as it contains intersecting loops. (c) Two examples of the scar states, which appear as a foliation of parallel loops in the dual picture. (d) Two examples of states that can be reached by the upper state in (c) by simultaneously flipping all spins in the dashed boxes. All configurations in (b), (c), and (d) represent parts of an infinite system.

near-term experiments with synthetic quantum matter. If the constraint is imposed as a hard constraint, as is usual in the study of scars [4–7], then the ergodicity breaking is exact.

*Model.*—We consider a model of spin-1/2 particles on an  $L \times L$  two-dimensional square lattice. We take periodic boundary conditions in both directions and assume that  $L$  is a multiple of 4 [22]. We use the notation  $X, Z$  for the Pauli  $X$  and  $Z$  operators, and denote the basis of  $Z$  by the states  $|0\rangle, |1\rangle$ . The spins interact according to the following Hamiltonian,

$$H(h) = -J \sum_{ijkl \in \square} \text{CZ}_{ij} \text{CZ}_{jk} \text{CZ}_{kl} \text{CZ}_{il} - h \sum_i X_i. \quad (1)$$

Therein,  $ijkl \in \square$  represents a set of four spins around a given plaquette (face) of the lattice, ordered clockwise and  $J > 0$ . The operator  $\text{CZ} = \mathbb{1} - 2|11\rangle\langle 11|$  is the two-body controlled- $Z$  operator, which is diagonal in the  $Z$  basis, and gives a minus sign when the two spins are both in the state  $|1\rangle$ . Let us denote  $\text{CZ}_p = \text{CZ}_{ij} \text{CZ}_{jk} \text{CZ}_{kl} \text{CZ}_{il}$  for  $i, j, k, l$  being the four sites around plaquette  $p$ . The  $\text{CZ}_p$  interaction can be viewed as a generalized Rydberg interaction. In atomic Rydberg arrays, two neighboring atoms experience a strong energy shift when they are both in the excited state ( $|1\rangle$ ) [23]. This phenomenon, known as the Rydberg blockade, is equivalent to an interaction by the term  $\text{CZ}_{ij}$  for each neighboring pair  $i, j$ , up to a constant shift. In contrast,  $\text{CZ}_p$  gives an energy shift only if there is an odd number of neighboring sites in the excited state (“neighboring 1’s”) around a given plaquette. Therefore,

we have a four-spin parity-dependent interaction which is similar to, but distinct from, the usual two-spin Rydberg interaction. This interaction can equivalently be expressed in terms of two- and four-body Ising interactions,  $\text{CZ}_p = \frac{1}{2}(\mathbb{1} + Z_i Z_k + Z_j Z_l - Z_i Z_j Z_k Z_l)$ .

The Hamiltonian in Eq. (1) has a  $\mathbb{Z}_2 \times \mathbb{Z}_2$  symmetry generated by flipping all spins on the even or odd sublattice of the square lattice [a site  $i = (x, y)$  is on the even (odd) sublattice if  $x + y$  is even (odd)]. Because of this, the interaction  $\text{CZ}_p$  depends only on the domain wall variables of the two sublattices. We therefore need only keep track of these domain wall variables [Fig. 1(a)]. The domain walls form two independent sets of closed loops on the two independent sublattices, and the two species of domain wall can intersect with one another on the plaquettes. On each plaquette, there can be no domain wall, a single domain wall between either the odd or the even sites, or a domain wall between both odd and even sites. This gives an effective four-dimensional Hilbert space on each plaquette [Fig. 1(a)]. The interaction  $\text{CZ}_p$  acts diagonally on this Hilbert space and gives a factor of  $-1$  when there are two domain walls present, i.e., when there is a crossing of loops, and otherwise does nothing. The spin-flip term  $\propto \sum_i X_i$  acts in this dual Hilbert space by fluctuating closed-loop configurations locally. This dual picture will be very helpful to visualize the frozen states that we describe in the next section, and to understand their robustness.

*Exponentially many perfect scars.*—We now consider the limit  $J \gg h$ . In this limit, the number of domain wall intersections becomes an emergent  $U(1)$  conserved quantity [24], up to a prethermal timescale exponentially [25]

long in  $J/h$  [20]. We work in the emergent symmetry sector with no intersections, i.e.,  $\text{CZ}_p = 1$  for all plaquettes  $p$ . This symmetry sector is spanned by product states that have an even number of pairs of neighboring 1's around every plaquette. Allowed and disallowed configurations are shown in Figs. 1(a) and 1(b). This symmetry sector is exponentially large in system volume; at the very least, if we put all spins on the even sublattice in the state  $|0\rangle$ , the state will be in the ground space regardless of the configuration of the odd sublattice, since there will be no neighboring 1's. This means the symmetry sector is capable of hosting volume-law entangled eigenstates. A more quantitative estimate of the sector size is provided by a Pauling estimate [29]. For a given plaquette, 12 of the possible 16 states are permitted by the no-crossing constraint. Once the constraints on adjacent plaquettes are also taken into account (on average), one finds  $N_0 \sim 2^{L^2} (12/16)^{L^2} = (3/2)^{L^2}$  states. This scaling is in good agreement with exact numerical enumeration of states [30].

Let us treat  $\text{CZ}_p = 1$  as a hardcore constraint that defines a restricted Hilbert space. This approximation becomes asymptotically exact in the prethermal limit  $h/J \rightarrow 0$ . To lowest order in perturbation theory, the effect of the magnetic field projected onto this restricted space is

$$H_0 = -h \sum_i X_i (P_i^{0000} + P_i^{1111}), \quad (2)$$

where  $P_i^{0000}$  projects the four sites neighboring  $i$  onto the state  $|0\rangle$ , and similarly for  $P_i^{1111}$ . This effective Hamiltonian strongly resembles that of PXP models [6,36–39], which arise as effective models in the presence of the Rydberg blockade. PXP models have dynamics given by constrained spin flips, where a spin can only flip if all of its neighbors are in the state  $|0\rangle$ . Here, we additionally allow the spin flip if all neighboring spins are in the state  $|1\rangle$ . This is a consequence of our parity-sensitive interaction in Eq. (1), since, while the latter spin flip creates new neighboring 1's (which is not allowed in the conventional Rydberg setup), it conserves the parity of neighboring 1's around each plaquette. As discussed in Ref. [40], the same lowest-order effective Hamiltonian  $H_0$  can be obtained using conventional Rydberg interactions with more than one degree of freedom per lattice site [41].

The PXP models are prototypical examples of models that host quantum many-body scars [42–44]. Similarly, the effective Hamiltonian  $H_0$  (2) also has scars. We remark that the eigenstates of  $H_0$  are related to those of  $H$  via a unitary basis transformation (the Schrieffer-Wolff transformation). We work in the basis of  $H_0$ , since here the scars are simple product states where each site has some neighbors in the state  $|0\rangle$  and some in the state  $|1\rangle$  [45]. Two such states are pictured in Fig. 1(c). Because no spins are flippable, these states are energy 0 eigenstates of  $H_0$ . Since  $H_0$  is mapped to  $-H_0$  by the global application of  $Z$ , energy 0 is exactly in the middle of the spectrum of  $H_0$  [46]. Despite this, these

states have no entanglement, as they are simply product states, which violates the expectation that states in the middle of the spectrum should have large entanglement. Therefore, we may call them examples of many-body scars. In the dual picture of domain walls, these states look like “foliations” of parallel noncontractible loops, as shown in Fig. 1(c). Because the loops are densely packed, no loop can fluctuate without creating intersections with its neighboring loops, which would violate our emergent (prethermal) conservation law.

The states pictured in Fig. 1(c) are not the only scar states in this model. In fact, the number of orthogonal scar states grows *exponentially* in linear system size  $L$ . The other scar states can be constructed in the following way. Observe that the states pictured in Fig. 1(c) consist of the repeated pattern “0011” along every row. In the first row, we can choose to shift this pattern in one of four ways. On each subsequent row, we can independently choose to shift the pattern left or right by one site with respect to the previous row. This generates  $2^{L+1}$  states. Rotating the lattice by  $90^\circ$  gives  $2^{L+1}$  additional states, but they are not all new states. Taking the repeated states into account, there are  $2^{L+2} - 8$  scar states in total. The graphical construction makes it clear that these states are all energy 0 eigenstates of  $H_0$ , and that they are all in the  $\text{CZ}_p = 1$  sector. In the dual picture, the different scar states come from different ways of putting kinks into the foliated loop pattern.

*Absolute robustness of the scar states.*—We have shown that, to the lowest order in perturbation theory, we can construct  $\sim 2^L$  scar states that have no entanglement and lie in the middle of the energy spectrum. Now, we consider higher orders in perturbation theory. To do this, we need to consider the possibility of a sequence of spin flips that temporarily violates the  $\text{CZ}_p = 1$  constraint before returning to an allowed state. The dual picture makes it clear that such a process does not exist to *any* finite order in perturbation theory. This is because every fluctuation of loops that is contained within a region with finite radius will inevitably create loop intersections within that region, or its boundary, due to the dense packing of loops. The only process that is allowed is one which pairwise annihilates two loops, or one which puts a kink in all loops across the entire system, see Fig. 1(d). We remark that the former process maps the scar state to a state which can now be acted on by local spin flips [upper state in Fig. 1(d)], while the latter maps to another scar state [lower state in Fig. 1(d)]. Both processes require simultaneously flipping a number of spins that is proportional to the linear system size  $L$ , so they only occur at an order of perturbation theory that is also proportional to  $L$ . Therefore, we say that the scar states pictured in Fig. 1(c) are robust to all finite orders in perturbation theory. We give a more rigorous argument of this robustness in Supplemental Material (SM) [30].

Remarkably, these scar states are also robust to arbitrary perturbations of the Hamiltonian. That is to say, in the

thermodynamic limit, the scar states will remain eigenstates even in the presence of arbitrary perturbations  $V$ , in the prethermal limit  $\tilde{h}/J \rightarrow 0$ , where  $\tilde{h}$  is the generalized perturbation strength. We start by noting that, in the prethermal limit, the perturbation must be projected into the symmetry sector with no domain wall intersections. We have already shown that the scar states are an energy 0 eigenstate of  $X$  or finite product of  $X$  operators, after such projection. On the other hand, since the scar states are product states in the  $Z$  basis, they will be eigenstates of any perturbation consisting of  $Z$  operators. We note that, unlike the  $X$ -type perturbations, the  $Z$ -type perturbations will shift the energy of the scar states away from 0. Since  $V$  can always be decomposed into products of  $X$ 's,  $Z$ 's, we see that the scars are indeed eigenstates of  $V$  after projection onto the prethermal symmetry sector. We emphasize that we have *not* required the perturbations to be symmetry restricted, or to have compact support—our proof carries through unchanged for perturbations that have long-range tails, and even for perturbations that are fully geometrically nonlocal, as long as they are  $k$  body with  $k/L \rightarrow 0$  in the thermodynamic limit.

We now address the convergence of perturbation theory. We note that  $-\sum_p \mathbf{CZ}_p$  has integer spectrum (we are working in the ground space thereof), so we can directly apply the rigorous theory of prethermalization [20,26–28]. This theory establishes that, while perturbation theory does not converge, the breakdown of perturbation theory in our model (as witnessed by local observables) only manifests beyond a prethermal timescale exponentially long in  $J/h$ . We contrast this with PXP-type models, where the analogous timescale is only polynomial in inverse perturbation strength [47].

*Intermediate Krylov sectors.*—Now, we investigate the existence of larger isolated sectors of Hilbert space. Instead of a dense packing of winding loops [Figs. 1(c) and 1(d)], consider the state depicted in the left panel of Fig. 2 which contains four adjacent noncontractible domain wall loops of alternating color surrounded by the domain wall vacuum. Under *local* dynamics, these loops can fluctuate, subject to the no-crossing constraint, and contractible loops can be created or destroyed from or into the vacuum, as depicted in the right panel of Fig. 2. Crucially, the no-crossing constraint implies that the number of noncontractible loops of alternating color remains an emergent constant of motion, since two loops of the same color cannot be pairwise annihilated without creating intersections with the loop in between them. More generally, intermediate sectors of Hilbert space can arise from some number of noncontractible loops that wind around any one of the horizontal, vertical, diagonal, or antidiagonal directions of the torus.

These intermediate sectors of Hilbert space can be understood as symmetry sectors of a  $U(1)$  1-form symmetry

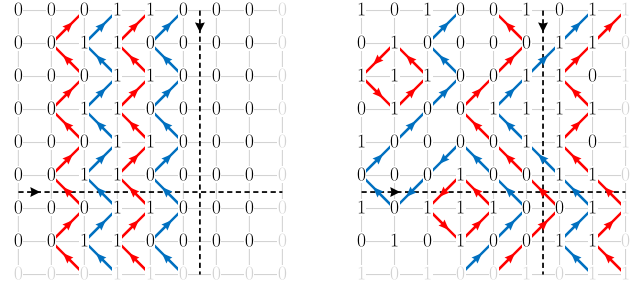


FIG. 2. A configuration of spins belonging to one of the “intermediate” sectors. Here, we take an  $8 \times 8$  lattice with periodic boundary conditions indicated by the gray numbers. The dashed lines indicate rows and columns along which  $Q_y$  and  $Q_x$ , respectively, are evaluated. In both cases, we have  $Q_y = 4$ ,  $Q_x = 0$ , implying these diagrams are in the same sector and are therefore related by a series of local moves.

that emerges due to the  $\mathbf{CZ}_p = 1$  constraint. To identify this symmetry, we refine the duality mapping from spins to loops to give the loops a well-defined orientation [30]. Examples of oriented loop patterns are pictured in Fig. 2. For any closed and oriented path  $P$  between plaquette centers, we can then compute the net flux  $Q_P$  of loops crossing  $P$ , where a sign convention can be fixed using the right-hand rule. Any contractible loop will necessarily intersect  $P$  twice (in opposite directions) and therefore will not contribute to the net flux. However, if  $P$  winds around a noncontractible path on the torus, it is possible for a noncontractible loop to intersect it only once. In particular, if we define  $Q_x$  and  $Q_y$  as the net flux across a noncontractible path along column  $x$  and row  $y$ , as depicted in Fig. 2, then  $|Q_x|$  ( $|Q_y|$ ) counts the number of loops that wind around the horizontal (vertical) direction of the torus. Importantly, a pair of adjacent noncontractible loops of the same color have opposite orientations. Therefore, only the loops of alternating color, which cannot be annihilated by local dynamics without introducing crossings, will contribute to  $Q_{x/y}$ . If a domain wall loop winds diagonally around the torus, it will contribute to both  $Q_x$  and  $Q_y$ . Since  $Q_P = 0$  for any contractible path  $P$ , the paths along which  $Q_{x/y}$  are evaluated can be arbitrarily locally deformed without changing their value, hence they should be considered 1-form symmetry charges.

Geometrically, it is clear that local fluctuations in the domain walls cannot change  $Q_{x/y}$ , so they are constants of motion. Small-scale numerical studies of the connectivity of Hilbert space under the dynamics of  $H_0$  support the claim that the magnitude and sign of  $Q_{x/y}$  uniquely label *all* intermediate sectors of Hilbert space, where domain walls are not fully packed [30]. These sectors can thus be viewed as symmetry sectors of the emergent one-form symmetry. However the scar states cannot be viewed in this way, as there are indeed only  $\sim L$  different values of  $Q_{x/y}$ , whereas the number of scar states is  $\sim \exp(L)$ . Therefore, the  $U(1)$

1-form symmetry sectors are *not* sufficient to uniquely label all the fragments of Hilbert space. Finally, we note that this  $U(1)$  1-form symmetry is indeed an *emergent* symmetry in the  $\mathbf{CZ}_p = 1$  sector, as loop crossings turn out to act as sources or sinks of oriented flux [30].

*Hydrodynamics.*—We now discuss dynamics from simple nonscar initial states. Within the  $\mathbf{CZ}_p = 1$  sector we show (see SM [30]) that this is well described by magnetohydrodynamics of the emergent one-form  $U(1)$  symmetry [48]. This analytic expectation may be confirmed using the automaton Monte Carlo technique [49] and single spin flip dynamics. Meanwhile, in sectors with intersections (a non-zero number of  $\mathbf{CZ}_p = -1$ ) we find that, starting from an “infinite temperature” initial condition, the long-time limit of the subsequent dynamics is characterized by isotropic diffusion of the intersections, which (we recall) are conserved up to the prethermal timescale [30].

*Conclusions.*—We have shown how a “generalized Rydberg constraint” can lead to an exponential number of frozen configurations (scars) which are provably robust to arbitrary  $k$ -local perturbations. Our results provide a new avenue for the design of ergodicity breaking models, which may function as robust memories, and may also be accessible in near-term quantum simulators [40]. Most broadly, they may prompt a reevaluation of the necessary desiderata for ergodicity breaking.

R. N. and O. H. are supported by the Air Force Office of Scientific Research under Award No. FA9550-20-1-0222. R. N. also thanks the Simons Foundation for a Simons Fellowship in Theoretical Physics. D. T. S. is supported by the Simons Collaboration on Ultra-Quantum Matter, which is a grant from the Simons Foundation (651440).

---

[1] R. J. Baxter, *Exactly Solved Models in Statistical Mechanics* (Elsevier, New York, 2016).  
 [2] R. Nandkishore and D. A. Huse, Many-body localization and thermalization in quantum statistical mechanics, *Annu. Rev. Condens. Matter Phys.* **6**, 15 (2015).  
 [3] D. A. Abanin, E. Altman, I. Bloch, and M. Serbyn, Colloquium: Many-body localization, thermalization, and entanglement, *Rev. Mod. Phys.* **91**, 021001 (2019).  
 [4] N. Shiraishi and T. Mori, Systematic construction of counterexamples to the eigenstate thermalization hypothesis, *Phys. Rev. Lett.* **119**, 030601 (2017).  
 [5] S. Moudgalya, N. Regnault, and B. A. Bernevig, Entanglement of exact excited states of Affleck-Kennedy-Lieb-Tasaki models: Exact results, many-body scars, and violation of the strong eigenstate thermalization hypothesis, *Phys. Rev. B* **98**, 235156 (2018).  
 [6] C. J. Turner, A. A. Michailidis, D. A. Abanin, M. Serbyn, and Z. Papić, Weak ergodicity breaking from quantum many-body scars, *Nat. Phys.* **14**, 745 (2018).  
 [7] A. Chandran, T. Iadecola, V. Khemani, and R. Moessner, Quantum many-body scars: A quasiparticle perspective, *Annu. Rev. Condens. Matter Phys.* **14**, 443 (2023).

[8] S. Pai, M. Pretko, and R. M. Nandkishore, Localization in fractonic random circuits, *Phys. Rev. X* **9**, 021003 (2019).  
 [9] V. Khemani, M. Hermele, and R. Nandkishore, Localization from Hilbert space shattering: From theory to physical realizations, *Phys. Rev. B* **101**, 174204 (2020).  
 [10] P. Sala, T. Rakovszky, R. Verresen, M. Knap, and F. Pollmann, Ergodicity breaking arising from Hilbert space fragmentation in dipole-conserving Hamiltonians, *Phys. Rev. X* **10**, 011047 (2020).  
 [11] S. Moudgalya, A. Prem, R. Nandkishore, N. Regnault, and B. A. Bernevig, Thermalization and its absence within Krylov subspaces of a constrained Hamiltonian, in *Memorial Volume for Shoucheng Zhang* (World Scientific, Singapore, 2022), pp. 147–209.  
 [12] T. Rakovszky, P. Sala, R. Verresen, M. Knap, and F. Pollmann, Statistical localization: From strong fragmentation to strong edge modes, *Phys. Rev. B* **101**, 125126 (2020).  
 [13] Z.-C. Yang, F. Liu, A. V. Gorshkov, and T. Iadecola, Hilbert-space fragmentation from strict confinement, *Phys. Rev. Lett.* **124**, 207602 (2020).  
 [14] A. Khudorozhkov, A. Tiwari, C. Chamon, and T. Neupert, Hilbert space fragmentation in a 2D quantum spin system with subsystem symmetries, *SciPost Phys.* **13**, 098 (2022).  
 [15] S. Moudgalya and O. I. Motrunich, Hilbert space fragmentation and commutant algebras, *Phys. Rev. X* **12**, 011050 (2022).  
 [16] A. Yoshinaga, H. Hakoshima, T. Imoto, Y. Matsuzaki, and R. Hamazaki, Emergence of Hilbert space fragmentation in Ising models with a weak transverse field, *Phys. Rev. Lett.* **129**, 090602 (2022).  
 [17] O. Hart and R. Nandkishore, Hilbert space shattering and dynamical freezing in the quantum Ising model, *Phys. Rev. B* **106**, 214426 (2022).  
 [18] J. Z. Imbrie, On many-body localization for quantum spin chains, *J. Stat. Phys.* **163**, 998 (2016).  
 [19] D. Sels and A. Polkovnikov, Dynamical obstruction to localization in a disordered spin chain, *Phys. Rev. E* **104**, 054105 (2021).  
 [20] D. Abanin, W. De Roeck, W. W. Ho, and F. Huveneers, A rigorous theory of many-body prethermalization for periodically driven and closed quantum systems, *Commun. Math. Phys.* **354**, 809 (2017).  
 [21] C. W. von Keyserlingk, V. Khemani, and S. L. Sondhi, Absolute stability and spatiotemporal long-range order in Floquet systems, *Phys. Rev. B* **94**, 085112 (2016).  
 [22] With open boundary conditions, the scars that we identify can melt from the corners inwards. If  $L$  is not divisible by four then the dense packing needed for perfect scars that we describe cannot be attained, although fragmentation may still occur.  
 [23] A. Browaeys and T. Lahaye, Many-body physics with individually controlled Rydberg atoms, *Nat. Phys.* **16**, 132 (2020).  
 [24] More precisely, the number of intersections is only conserved up to a quantity of order  $\sim h/J$ .  
 [25] For perturbations decaying slower than some critical power law [26–28], the prethermal timescale may be modified.

- [26] W. W. Ho, I. Protopopov, and D. A. Abanin, Bounds on energy absorption and prethermalization in quantum systems with long-range interactions, *Phys. Rev. Lett.* **120**, 200601 (2018).
- [27] F. Machado, G. D. Kahanamoku-Meyer, D. V. Else, C. Nayak, and N. Y. Yao, Exponentially slow heating in short and long-range interacting Floquet systems, *Phys. Rev. Res.* **1**, 033202 (2019).
- [28] F. Machado, D. V. Else, G. D. Kahanamoku-Meyer, C. Nayak, and N. Y. Yao, Long-range prethermal phases of nonequilibrium matter, *Phys. Rev. X* **10**, 011043 (2020).
- [29] L. Pauling, The structure and entropy of ice and of other crystals with some randomness of atomic arrangement, *J. Am. Chem. Soc.* **57**, 2680 (1935).
- [30] See Supplemental Material at <http://link.aps.org/supplemental/10.1103/PhysRevLett.132.040401> for a discussion of (i) the augmented duality mapping, (ii) a discussion of the model's relaxation towards equilibrium, and (iii) a discussion of the Schrieffer-Wolff transformation to the rotated basis in which the scars are maximally simple, and of the nontrivial dynamics arising in the 'bare' basis, which includes Refs. [31–35].
- [31] J. Feldmeier, P. Sala, G. De Tomasi, F. Pollmann, and M. Knap, Anomalous diffusion in dipole- and higher-moment-conserving systems, *Phys. Rev. Lett.* **125**, 245303 (2020).
- [32] J. Iaconis, A. Lucas, and R. Nandkishore, Multipole conservation laws and subdiffusion in any dimension, *Phys. Rev. E* **103**, 022142 (2021).
- [33] C. L. Henley, The “Coulomb phase” in frustrated systems, *Annu. Rev. Condens. Matter Phys.* **1**, 179 (2010).
- [34] C. Castelnovo, R. Moessner, and S. Sondhi, Spin ice, fractionalization, and topological order, *Annu. Rev. Condens. Matter Phys.* **3**, 35 (2012).
- [35] X. Chen, R. M. Nandkishore, and A. Lucas, Quantum butterfly effect in polarized Floquet systems, *Phys. Rev. B* **101**, 064307 (2020).
- [36] I. Lesanovsky and H. Katsura, Interacting fibonacci anyons in a Rydberg gas, *Phys. Rev. A* **86**, 041601(R) (2012).
- [37] C. J. Turner, A. A. Michailidis, D. A. Abanin, M. Serbyn, and Z. Papić, Quantum scarred eigenstates in a Rydberg atom chain: Entanglement, breakdown of thermalization, and stability to perturbations, *Phys. Rev. B* **98**, 155134 (2018).
- [38] A. A. Michailidis, C. J. Turner, Z. Papić, D. A. Abanin, and M. Serbyn, Stabilizing two-dimensional quantum scars by deformation and synchronization, *Phys. Rev. Res.* **2**, 022065(R) (2020).
- [39] C.-J. Lin, V. Calvera, and T. H. Hsieh, Quantum many-body scar states in two-dimensional Rydberg atom arrays, *Phys. Rev. B* **101**, 220304(R) (2020).
- [40] A. Celi, B. Vermersch, O. Viyuela, H. Pichler, M. D. Lukin, and P. Zoller, Emerging two-dimensional gauge theories in Rydberg configurable arrays, *Phys. Rev. X* **10**, 021057 (2020).
- [41] Although the lowest-order Hamiltonian is reproduced in Ref. [40], the robustness to higher-orders which we describe shortly will presumably be absent.
- [42] M. Serbyn, D. A. Abanin, and Z. Papić, Quantum many-body scars and weak breaking of ergodicity, *Nat. Phys.* **17**, 675 (2021).
- [43] Z. Papić, Weak ergodicity breaking through the lens of quantum entanglement, in *Entanglement in Spin Chains: From Theory to Quantum Technology Applications*, edited by A. Bayat, S. Bose, and H. Johannesson (Springer International Publishing, Cham, 2022), pp. 341–395.
- [44] S. Moudgalya, B. A. Bernevig, and N. Regnault, Quantum many-body scars and Hilbert space fragmentation: A review of exact results, *Rep. Prog. Phys.* **85**, 086501 (2022).
- [45] Due to the Schrieffer-Wolff transformation, the true eigenstates of  $H$  are not product states but will nonetheless have low entanglement that vanishes with  $h/J$ , see [30].
- [46] We can furthermore show that the ground state of  $H_0$  has finite energy density using a variational argument: The state with  $|+\rangle = (1/\sqrt{2})(|0\rangle + |1\rangle)$  on even vertices and  $|0\rangle$  on odd vertices has  $\langle X_i(P_i^{000} + P_i^{111}) \rangle = \frac{1}{2}$  on average. Therefore, the true ground state has energy  $E < -hL^2/2$ .
- [47] C.-J. Lin, A. Chandran, and O. I. Motrunich, Slow thermalization of exact quantum many-body scar states under perturbations, *Phys. Rev. Res.* **2**, 033044 (2020).
- [48] M. Qi, O. Hart, A. J. Friedman, R. Nandkishore, and A. Lucas, Hydrodynamics of higher-rank gauge theories, *SciPost Phys.* **14**, 029 (2023).
- [49] J. Iaconis, S. Vijay, and R. Nandkishore, Anomalous subdiffusion from subsystem symmetries, *Phys. Rev. B* **100**, 214301 (2019).